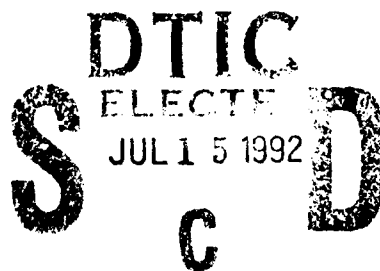


AD-A253 687



2

PL-TR-92-2037

UWY/AP-91/1216

# AEROSOL OPTICAL PROPERTIES OF THE FREE TROPOSPHERE

James M. Rosen

Department of Physics & Astronomy  
University of Wyoming  
Laramie, Wyoming 82071

16 December 1991

Scientific Report No. 2

APPROVED FOR PUBLIC RELEASE: DISTRIBUTION UNLIMITED.

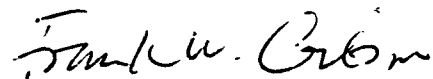


PHILLIPS LABORATORY  
AIR FORCE SYSTEMS COMMAND  
HANSCOM AIR FORCE BASE, MASSACHUSETTS 01731-5000

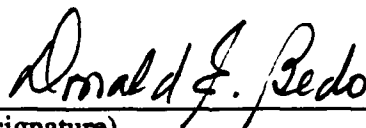
92-18393



This technical report has been reviewed and is approved for publication.



(signature)  
Frank Gibson  
Contract Manager



(signature)  
Donald E. Bedo, Chief  
Electro-Optical Measurements



(Signature)  
Alan D. Blackburn, Col., USAF  
Director, Optical Environment Division

This document has been reviewed by the ESD Public Affairs Office (PA) and is releasable to the National Technical Information Service (NTIS).

Qualified requestors may obtain additional copies from the Defense Technical Information Center. All others should apply to the National Technical Information Service.

If your address has changed, or if you wish to be removed from the mailing list, or if the addressee is no longer employed by your organization, please notify PL/TSI, Hanscom AFB, MA 01731-5000. This will assist us in maintaining a current mailing list.

Do not return copies of this report unless contractual obligations or notices on a specific document requires that it be returned.

REPORT DOCUMENTATION PAGE			Form Approved OMB No. 0704-0188	
<small>This report has been prepared for the collection of information in response to a request, including the time for reviewing instructions, searching existing data sources, gathering and maintaining the data needed, and completing and reviewing the collection of information. Send comments regarding this burden estimate or any other aspect of this collection of information, including suggestions for reducing this burden, to Washington Headquarters Services, Directorate for Information Operations and Reports, 1215 Jefferson Davis Highway, Suite 1204, Arlington, VA 22202-4302, and to the Office of Management and Budget, Paperwork Reduction Project (0704-0188), Washington, DC 20503.</small>				
1. AGENCY USE ONLY (Leave blank)		2. REPORT DATE 16 December 1991		3. REPORT TYPE AND DATES COVERED Scientific No. 2
4. TITLE AND SUBTITLE  AEROSOL OPTICAL PROPERTIES OF THE FREE TROPOSPHERE			5. FUNDING NUMBERS  Contract F19628-90-K-0011 PE 62101F PR 7670 TA 15 WU AU	
6. AUTHOR(S)  James M. Rosen				
7. PERFORMING ORGANIZATION NAME(S) AND ADDRESS(ES)  Department of Physics and Astronomy University of Wyoming Laramie, WY 82071			8. PERFORMING ORGANIZATION REPORT NUMBER  UW/AP/91/1216	
9. SPONSORING / MONITORING AGENCY NAME(S) AND ADDRESS(ES)  Phillips Laboratory Hanscom AFB, MA 01731-5000 Contract Manager: Frank Gibson/OPA			10. SPONSORING / MONITORING AGENCY REPORT NUMBER  PL-TR-92-2037	
11. SUPPLEMENTARY NOTES				
12a. DISTRIBUTION / AVAILABILITY STATEMENT  Approved for public release; distribution unlimited			12b. DISTRIBUTION CODE	
13. ABSTRACT (Maximum 200 words)  <p>Nearly simultaneous measurements of the physical and optical properties of boundary layer and free tropospheric aerosols near Boulder, Colorado were made on several occasions using aircraft, balloon, and ground based sensors. This effort was conducted with the purpose of obtaining a diverse, self-consistent data set that could be used for testing optical model calculations based on measured physical characteristics such as apparent size distribution, composition, and shape. Support under this grant made it possible to perform a detailed analysis of this unique data set. It was found that even with the uncertainties involved, the model predictions are in good agreement with the measurements in the visible and near infrared wavelength regions. The results also indicate that during the measurement period the aerosol in the boundary layer and free troposphere behaved as spherical particles for optical modeling purposes. The utility of the observations for determining the extinction-to-backscatter ratio relevant to aerosols in the boundary layer and free troposphere is described with typical measured values being in the 20 to 30 sr range. Further data sets and analysis of this type will be made possible by using the specialized instrumentation developed at the University of Wyoming during the last year.</p>				
14. SUBJECT TERMS  Aerosol Scattering, Free Troposphere			15. NUMBER OF PAGES 24	
			16. PRICE CODE	
17. SECURITY CLASSIFICATION OF REPORT UNCLASSIFIED	18. SECURITY CLASSIFICATION OF THIS PAGE UNCLASSIFIED	19. SECURITY CLASSIFICATION OF ABSTRACT UNCLASSIFIED	20. LIMITATION OF ABSTRACT UNLIMITED	

# CONTENTS

INTRODUCTION .....	1
INSTRUMENTATION .....	1
Particle Counters .....	2
Impactor .....	2
CN Counter .....	2
Nephelometer .....	2
Aethalometer .....	3
Ruby Lidar .....	3
Backscattersonde .....	3
LOGISTICS OF THE EXPERIMENT .....	3
RESULTS .....	4
Comparison of Nephelometer and Backscattersonde .....	5
Aerosol Optical Model Calculations .....	5
Index of Refraction .....	6
Particle Shape .....	6
Size Distribution .....	7
DISCUSSION .....	8
CONCLUSIONS .....	8
REFERENCES .....	9
TABLES .....	12
FIGURES .....	13



Accession For	
DTIC	<input checked="" type="checkbox"/>
ORNL	<input type="checkbox"/>
NSF	<input type="checkbox"/>
Unpublished	<input type="checkbox"/>
Justification	
By	
Distribution/	
Availability Codes	
Dist	Avail and/or Special
A-1	

## SUMMARY

This year's research effort was centered around two areas of activity: the completion of optical devices to measure aerosol scattering along with their associated calibration mechanisms, and the analysis of data obtained in a unique field experiment of opportunity conducted in cooperation with several other investigators. Since most of the progress concerning the instrument development portion of the research was presented in the quarterly reports, this report will focus on the results and interpretation of the field measurements.

# **AEROSOL OPTICAL PROPERTIES OF THE FREE TROPOSPHERE**

## **Introduction**

The field program mentioned in the summary involved nearly simultaneous measurements of the physical and optical properties of boundary layer and free tropospheric aerosols near Boulder, Colorado using aircraft, balloon, and ground based sensors, and was conducted for the purpose of obtaining a diverse, self-consistent data set that could be used for testing optical model calculations based on measured physical characteristics such as apparent size distribution, composition, and shape.

Although the applicability of Mie scattering calculations to spherical aerosol particles of known size distribution and composition is on a solid theoretical foundation, very little is known of the applicability of the same calculations and assumptions when applied to real atmospheric aerosol polydispersions of poorly known particle shape and composition. The size distribution is a critical component in the Mie calculations and is often determined from measurements with optical particle counters, which in turn are calibrated and the data analyzed in terms of spherical particles of known composition. Thus, the size distribution determined in such a manner may be relatively meaningless for quantitative applications. An important question addressed in this report is the following: How accurate and reliable are the predictions of standard Mie scattering calculations when based on size distributions "measured" in the boundary layer and free troposphere with commonly used optical particle counters whose calibration and response is interpreted under the assumption of spherical particles?

The field measurements reported here were centered around obtaining a data set comprehensive enough to test quantitative aerosol scattering calculations and relationships for aerosols found throughout the troposphere. These measurements were made simultaneously (or quasi simultaneously) and involved observations of diverse aerosol properties using a variety of in situ airborne and ground based remote sensors.

The measurements took place on three evenings near Boulder, Colorado in a cooperative effort with several other research facilities. The first field observations were on July 26, 1989 and the second set of measurements took place on May 23 and 24, 1990. Two reports [Bodhaine et al., 1990, 1991a] present the basic and uninterpreted data obtained during these experiments.

## **Instrumentation**

There were four separate measurement systems involved: NOAA's instrumented King Air aircraft, a ruby lidar (694.3 nm) and the University of Wyoming balloon borne backscatter-sonde. The aircraft was under the direction of NOAA's Climate Monitoring and Diagnostics Laboratory (CMDL) and Air Resources Laboratory (ARL).

Both lidars were operated by NOAA's Wave Propagation Laboratory (WPL), and the balloon borne backscatter-sonde measurements were conducted by the University of Wyoming Atmospheric Physics Group (APG).

A detailed description and performance capabilities of the instrumentation and sensors employed in the experiment has been given by Bodhaine et al. [1991a, 1990]. The general

nature of the aircraft platform has been given by Wellman et al. [1989]. Therefore, only an abbreviated description of the instrumentation is needed here.

### Particle Counters

The optical particle counters (Particle Measuring Systems' laser particle spectrometers ASASP-100X and FSSP-100) are commercially available instruments in widespread use. Their application to the aircraft and calibration for various refractive indices has been discussed by Kim and Boatman [1990a, 1990b]. It should be noted that the sensing volume of the FSSP-100 probe is in the free air stream external to the aircraft and does not experience an-isokinetic sampling problems. However, its sampling rate is relatively small and in regions of low aerosol concentration, such as the free troposphere, the sample time required to obtain statistically significant data may become quite large. Unless otherwise noted, the ASASP and FSSP profiles utilized here employ 1 min averages.

### Impactor

The cascade impactor is a PIXE Corporation five stage single orifice device. The equivalent aerodynamic cutoff diameters (EACD's) for the five stages are as follows: stage 5,  $4\mu\text{m}$ ; stage 4,  $2\mu\text{m}$ ; stage 3,  $1\mu\text{m}$ ; stage 2,  $0.5\mu\text{m}$ ; stage 1,  $0.25\mu\text{m}$ . Although these cuts are altitude dependent, the effect is not important to the experiment, because the collections were only used to indicate the chemical composition for two gross size ranges: fine and coarse. Budgetary constraints limited analysis to stages 1, 3 and 5. The elemental composition of individual particles was determined through energy dispersive x-ray analysis, which was performed with an ultra thin window x-ray spectrometer interfaced with an analytical electron microscope. With this spectrometer, light elements such as carbon and oxygen are observable in individual atmospheric particles. More details concerning the operation of this sampling device, its application to the aircraft and the analysis of the collected aerosol is given by Sheridan et al. [1991].

### CN Counter

The General Electric condensation nucleus (CN) counter (model 112L428G1) is a modified version of a commercially available instrument in relatively widespread use [Bodhaine and Murphy, 1980]. Because of the potential possibility of air leaks in this sensor, it must be operated at aircraft cabin pressure. This was accomplished by employing an air sample compressor device ahead of the instrument. Laboratory experiments indicate that a loss of about 20% in CN concentration can be attributed to the compressor. The data shown here have been corrected for this loss. The particle sizes detected by this instrument are roughly  $0.01\mu\text{m}$  and larger.

### Nephelometer

The operation, characteristics, and calibration of the three wavelength nephelometer (449, 536 and 690 nm) have been described in detail by Bodhaine et al. [1991b]. For the aircraft application, an air inlet and downstream pump with air exhaust to the outside of the aircraft provides about 200 LPM airflow through the nephelometer and allows operation at ambient pressure regardless of aircraft cabin pressurization. Air pressure and temperature measurements made inside the nephelometer make it possible to apply a small correction to obtain the true ambient scattering characteristics. The data have not been corrected for possible loss of particles in the intake tube by processes such as sedimentation, impaction,

and evaporation. In the vertical profiles reported here, the nephelometer data have been averaged for 10 seconds giving an effective vertical resolution of about 22 meters.

The particular nephelometer employed in the experiment integrates the scattered light over the angles  $7^{\circ}$ -  $170^{\circ}$ . Since the amount of light scattered into the  $0^{\circ}$ - $7^{\circ}$  and  $170^{\circ}$ - $180^{\circ}$  angular region is relatively small for the particle sizes encountered, the nephelometer provides a measure of the total aerosol scattering which is equivalent to the extinction if the particles are non absorbing (no imaginary component in the index of refraction).

#### Aethalometer

The Aethalometer (Hansen and Rosen, 1984) was specially constructed for application on the NOAA King Air aircraft. This instrument uses a light diffusing filter that continuously accumulates aerosol while illuminated by a lamp. Two photocells measure the intensity of the light from two portions of the filter: one is the sample signal from the area where aerosol is accumulating, and the other is a reference signal from an area where no aerosol is accumulating. Only the absorbing component (imaginary part of the index refraction) will contribute to a reduction of intensity in the sample beam. The decrease in the ratio of the sample to reference beam intensities as a function of time is calibrated in terms of the equivalent concentration of carbon being drawn through the filter, and a value is reported every 10 seconds. A large pump pulls air through the filter at a measured flow rate exceeding 30 LPM. The exhaust line from the pump is routed directly to the outside of the aircraft. The aethalometer measured aerosol absorption during both flights of the May 1990 experiment, but was not employed in the July 26, 1989 experiment.

#### Ruby Lidar

The ruby lidar system, operating at 694 nm wavelength, has been in intermittent use at Boulder, Colorado for a period of about 20 hr and is employed primarily for the monitoring of stratospheric aerosols. It transmits one pulse once every 3 seconds and typically requires an average of several hundred pulses to retrieve a statistically significant backscatter profile. Thus a profile can be obtained about every 10 minutes. The problems associated with the calibration of ruby lidar systems and the methodology of data analysis have been discussed by Russell et al. [1979] and by Likura et al. [1987].

#### Backscattersonde

The backscattersonde is a simple and relatively new balloon borne sensor. It employs a quasi collimated beam from a xenon flash lamp and sense the light locally backscattered at two selectable wavelengths. One vertical profile with a resolution of about 30 m (as determined by the flash lamp frequency and balloon rise rate) is obtained on ascent. During the field measurements, one of the backscatter wavelengths was always chosen to be 940 nm and the second wavelength was selected as either 700 (26 July 1989, 23 May 1990) or 480 nm (24 May 1990). Standard meteorological parameters (pressure, temperature and humidity) are also measured with a modified Vaisala radiosonde under microprocessor control, which is an integral part of the sounding instrument. A more complete description of the instrument and its calibration is given by Rosen and Kjöme [1991].

#### Logistics of the Experiment

On a typical experiment evening, the ruby lidar would start operation shortly after local sunset and continue obtaining profiles at 30 min intervals until undisturbed profiles were



consistently obtained under relatively cloud free conditions. At this time the aircraft took off from a local airport and began collecting data on a uniform ascent to about 400 mb (about 7 km).

The balloon launch was scheduled so that its ascent and that of the aircraft would approximately coincide. Obvious physical and practical constraints did not permit the respective profiles to be taken from exactly the same air parcels. However, since the atmospheric conditions were relatively stable as determined by comparisons of ascent and descent profiles, the effect of this deficiency is probably not significant for most parts of the profiles.

## Results

Particle concentration profiles obtained during the first field experiment for three typical particle sizes and for CN are shown in Figure 1. These results illustrate the diverse profiles that can be obtained in various size ranges. For example, the profile associated with particle diameter =  $0.57 \mu\text{m}$  shows a layer near 500 mb which is not evident in the smaller particle profile and appears as a layer deficient in concentration for the larger particles. The structure in the CN profile seems relatively uncorrelated with the larger particle profiles and does not show a decrease in concentration above the boundary layer as defined by the location of the temperature inversion. It is not immediately obvious at this point what the net contribution is of particles in and near the 500 mb layer to the optical scattering characteristics: Will this be a layer of relatively low or high scattering characteristics?

Figure 2 presents similar results for the second field experiment but includes the black carbon concentration profile and a comparison of ascent/descent profiles. Again, some corresponding features are evident in both the particle counter and CN profiles, but there are also many significant differences so that it would appear to be impossible to deduce one of the profiles given the others. The structure in the black carbon profile is not strongly correlated with features in the particle profiles and does not show the distinctive sharp decrease above the boundary layer. Thus, it is not possible to clearly associate the particles containing black carbon with a specific particle size profile.

Some notable differences in the ascent and descent structures can be seen in Figure 2. The particle concentration profiles on both May 23 and 24 show some differences near and at the top of the boundary layer (about 500 mb). These differences are thought to be real and probably reflect modest changes in the atmospheric conditions. The apparent shift in altitude of the ascent and descent CN profiles is undoubtedly an artifact probably due to a lag time associated with a delay of the air sample reaching the sensor. The systematic difference between the ascent and descent black carbon profiles at low concentrations is now known to be an instrument artifact caused by a pressure change rate effect on the filter opacity. To a first approximation, the correct black carbon concentration would be the average of the ascent and descent data.

Figure 3 shows a comparison of the particle concentration profiles and the various optical scattering profiles. To be consistent and for ease of comparison, mixing ratio units have been used for the aerosol concentration. The nephelometer and backscattersonde aerosol scatter ratio (aerosol/Rayleigh) is effectively a mixing ratio. Another often used quantity (which is not a mixing ratio) is the nephelometer and backscattersonde scatter ratio: (aerosol + Rayleigh)/Rayleigh. Note that aerosol scatter ratio = scatter ratio - 1.

All of the profiles in Figure 3 refer to the time period of aircraft and balloon ascent except for 23 May. Since the nephelometer was not operating during ascent on this date,

only aircraft descent profiles are shown.

Figure 3 shows excellent agreement in the fine profile structure as obtained with the nephelometer and backscattersonde, even though each instrument is sensitive to different aerosol scattering properties. The aerosol particle concentration profiles have somewhat lower resolution, but nevertheless reflect the same structure as seen with the nephelometer and backscattersonde. The lidar profiles as illustrated are significantly lower in vertical resolution, but are generally consistent with the structure shown in the other aerosol scattering measurements.

Although there is only modest agreement in the backscattersonde and ruby lidar profile structure in the troposphere, the general shape of the complete profile and agreement in absolute value appear to be quite satisfactory, as illustrated in Figure 4. Here, two ruby lidar profiles obtained on 23 May during balloon ascent are shown along with the tropospheric backscattersonde data at 700 nm wavelength. Unfortunately there was a balloon failure near 9 km on this date and no stratospheric data were observed. The backscattersonde data shown above 10 km in Figure 4 were obtained at Laramie, Wyoming (150 km north of Boulder) a few weeks later. However, the stratospheric aerosol was very stable during this period of time, and soundings made before and after the experiment showed very little difference in the stratosphere. Thus, it is believed that Figure 4 represents a valid comparison of the backscattersonde and ruby lidar over their entire operating altitude range.

Aerosol sampling with the 5 stage cascade impactor was performed over just two altitude ranges on both evenings of the second experiment: one sample was obtained in the planetary boundary layer and the other sample was collected in the free troposphere.

In the high and low altitude samples, about 85% of the fine particles (stage 1 collections) were classified as ammonium sulfate. Other particle groups were identified as composite sulfate/crustal (about 4%), crustal (about 5%), and carbonaceous/non-spherical (about 3%). The crustal group is rich in silicon and aluminum.

The coarse particle samples (stage 3 collections), did not show a consistent altitude dependent composition. Approximately 34% of the particles were classified as ammonium sulfate, 7% as composite sulfate/crustal, 43% as crustal, 5% as carbonaceous/non-spherical and 3 percent as iron-rich. A statistically significant number of particles were not collected on stage 5, but they appeared similar in composition to those collected on stage 3. More detail concerning the exact definition of the various groups such as crustal and carbonaceous has been given by Bodhane et al., 1991a.

Particles collected by the impactor in all of the samples were largely external mixtures of the dominant fine sulfates, some larger crustal derived particles and the less frequently encountered carbonaceous particles. Composite particles were observed, but typically near the 5% level.

#### Comparison of Nephelometer and Backscattersonde.

For the purpose of discussion below, the ratio of the nephelometer scatter ratio to the backscattersonde scatter ratio will be useful. In making this calculation, the profiles from the two sensors have been vertically shifted slightly so that there is optimal correspondence in the structure. This minor shift is probably a result of the samples not being made in exactly the same air parcel and a time lag in the effective response. Figure 5 shows the ratio of the instruments' response averaged over 2 mb altitude intervals. Data appear to be grouped in two regions of the chart which correspond to data from the planetary boundary layer (higher values) and from the free troposphere (lower values). A standard regression, straight

line fit has been performed using all of the data points, although a linear relationship is not necessarily expected. As the data points approach the origin (1,1) both instruments should read the same value, namely 1.00. Although the regression fit does pass reasonably close to the origin, there is a noticeable slight offset, but that is probably within the net experimental uncertainty. The straight line could be made to pass directly through the origin by adjusting or applying a small constant background signal to one or both of the instruments.

Much of the data scatter in Figure 5 can be attributed to points occurring near large gradients in vertical aerosol structure. In this situation, a small error in the corresponding corrected altitudes of the instrument platforms will lead to a relatively large error in the ratio of the response of the instruments. To address this problem in the May 1990 experiments, data were averaged over six well defined altitude regions or layers where the aerosol properties remained relatively constant. These layers are identified and numbered along the altitude scales in Figure 3. A comparison of the nephelometer and backscattersonde for the six layers on May 23 is shown in Figure 5. These data show less scatter and are consistent with an "eye fit" straight line passing through the origin. Backscattersonde data for 700 nm are not available for May 24.

The reader should be reminded that Figures 5 and 6 do not represent a universal relationship between the nephelometer and backscattersonde. The results apply only to the aerosol physical properties and vertical structure that existed during the field experiments. The measurements would need to be repeated many more times before an attempt could be made to identify a statistically significant result relating to atmospheric aerosols.

#### Aerosol Optical Model Calculations

Aerosol characteristics relevant to optical model calculations are size distribution, index of refraction as dictated by composition, and particle shape. An examination of how calculated model results are influenced by uncertainties in the input data is also important. Without an estimate of the uncertainties, it is impossible to assess the significance of the results or possible discrepancies that may occur between the measured and calculated quantities.

#### Index of Refraction

The observed dry aerosol composition as discussed above suggests an index of refraction in the range of  $1.50 \pm .03$  in the visible. Since the ambient relative humidity was well below 100% for most of the measurements, water incorporated in the particles probably did not significantly influence the index of refraction. The carbonaceous component of the sampled aerosol suggests a small absorbing component or imaginary part to the refractive index. The magnitude of the imaginary component can be estimated from the black carbon measurements. Table 1 suggests that black carbon made up about 2% of the total aerosol during the field measurements. Assuming that the black carbon has the same imaginary index of refraction as soot (which is approximately  $-.43i$  Kent et al., 1983) and using a simple minded volume averaged calculation, the first guess for the effective imaginary component for the aerosols should be roughly  $-.0086i$ . To be consistent with values in general use, we have chosen a slightly smaller value ( $-.006i$ ) [Kim and Boatman, 1990a; Kent et al., 1983] for initial calculations involving an absorbing component.

Rather than using a single value for the index of refraction, an ensemble of values has been chosen so that the sensitivity of the final results to the refractive index can be estimated. Table 2 gives a list of the indices considered as well as a suggested physical identification of

the aerosol based on the aerosol models of Shettle and Fenn [1979] and as further utilized by Kim and Boatman [1990a,b] and Kent et al. [1983].

### Particle Shape

As expected, electron microscope photographs indicate that the particles collected by the impactor were non-spherical [Bodhaine et al., 1991a]. On the other hand, the particles were not extremely irregular in shape. Thus, the calculations being performed here are probably not a severe test of the spherical particle assumption.

### Size Distribution

For both periods of the field experiments, size distributions were determined using the ASASP and FSSP instruments. The cascade impactor was not used for this purpose. Both of the optical particle counters were calibrated with spherical particles of known index of refraction. Since the response of these counters is well characterized, the calibration for spherical particles with other indices of refraction can be reliably calculated [Pinnick and Auvermann, 1979; Garvey and Pinnick, 1983; Kim and Boatman, 1990a,b].

Even though particle concentration information is available at one minute intervals or less, usually considerably more time is needed to obtain a statistically significant size distribution. For this reason, the size distribution has been determined for a few easily identifiable layers and regions as defined along the altitude scales in Figure 3. For reference, each layer has been numbered on each date starting at the highest layer. Average values of the aerosol physical and optical parameters have been computed for these layers.

An ensemble of possible size distributions is generated for each layer using the following procedure: To obtain one candidate size distribution, an index of refraction is selected (in sequence) from the ensemble of possible values and the corresponding particle counter calibration (channel number or response vs. size), assuming spherical particles, is then determined. A two mode log normal curve is fit to the resulting size distribution data using the technique described by Horvath et al., [1990] and the entire procedure is repeated for all of the indices of refraction in the ensemble. Three log normal parameters for each mode are obtained:  $N_o$  is the total particle concentration,  $D_g$  or  $r_g$  is the geometric mean diameter or radius, and  $\sigma_g$  is the geometric standard deviation defined such as that for a mono dispersed aerosol,  $\sigma_g = 1$ .

For each layer, using the ensemble of size distributions defined by the corresponding ensemble of refractive indices, the response of the nephelometer and backscatter sonde at the appropriate wavelengths were calculated using Mie scattering theory. The small dependence of index of refraction on wavelength has been neglected for these calculations. Since the backscatter sonde and ruby lidar are essentially equivalent, the ruby lidar backscatter has not been calculated.

For each layer and each index of refraction chosen, a set of calculated scattering values is obtained and can be compared with the measured values. As expected, some assumed refractive indices give better overall agreement with measurements than others. The values of refractive index giving the optimal simultaneous agreement with the nephelometer (3 values corresponding to 3 different wavelengths) and backscatter sonde (2 values corresponding to 2 different wavelengths) are shown in Table 3. Using these optimal values of refractive index, the overall comparison of model prediction and measurement is summarized in Figure 7. Each point in this figure is derived from a calculated and measured value for a given layer,

a particular instrument (backscattersonde or nephelometer), and for one of the possible wavelengths associated with the instrument.

## Discussion

Except for the imaginary or absorbing component, the optimal values of the refractive indices as shown in Table 3 are quite consistent with the range of values suggested from the chemical composition. The best results are obtained by neglecting the imaginary part of the refractive index, even though the aethalometer and impactor results indicate the presence of at least some absorbing aerosol. The estimates made above for the magnitude of this component are apparently too large and probably represent an upper limit. Our estimates of the index of refraction are consistent with those reported by Spinhirne et al. [1980] who have used a combination of optical methods to deduce a mean aerosol index of refraction for the boundary layer of  $1.52 - .003i$ .

The rather good agreement between calculated and measured optical properties as shown in Figure 7 is better than we initially anticipated and could be due to the fact that the aerosols were probably quasi spherical. The experiment would need to be repeated for a wider variety of aerosol conditions before a firm conclusion could be established. Nevertheless, the results of this work indicated that, at least under some conditions, aerosol optical properties in the boundary layer can be adequately estimated using size distributions obtained from optical particle counters.

The fact that reasonable agreement has been achieved for the comparisons shown in Figure 7 suggests that the spherical particle assumption does not necessarily lead to inaccurate results. Efforts to directly determine the response of the ASAP to uniform non-spherical particles (doublet spheres) indicate that the instrument responds to these particles as it would to spheres of equal volume [Pinnick and Rosen, 1979]. This earlier work also suggests that optical particle counters can produce meaningful results when applied to aerosol systems of non-spherical particles.

The high quality quasi simultaneous nephelometer and backscattersonde measurements obtained in the field measurements can be used to determine a very useful, but not well known, conversion factor that allows the derivation of optical depth from lidar profiles. This is the so called aerosol extinction-to-backscatter ratio frequently reported in units of  $\text{km}^{-1}/(\text{km}^{-1} \text{sr}^{-1})$  or sr. As mentioned above, the nephelometer is a measure of the extinction if there is no significant absorbing component to the particles, as was apparently the case for the observed aerosols. Figure 5 indicates an aerosol extinction-to-backscatter ratio (at about 700 nm) of 2.3 to 3.6 and Figure 6 indicates a value of 2.5. According to elementary scattering considerations these numbers need to be multiplied by  $8\pi/3$  (the Rayleigh extinction-to-backscatter ratio is  $24 \pm 6$  sr. For comparison, Spinhirne et al. [1980] have reported values of  $19.5 \pm 8.3$  sr for the mixed boundary layer at the same wavelength.

## Conclusions

The results of the work reported here suggest that optical particle counters can produce meaningful size distributions in a statistical sense for optical model calculations in the boundary layer and free troposphere, in spite of the fact that the particles are non-spherical. However, the limited amount of experience prevents this conclusion from being universal.

Combined soundings of the nephelometer and backscattersonde can lead to a relatively direct determination of the extinction to backscatter ratio. This ratio plays an important role in the interpretation and utility of data obtained by many remote sounding systems.

#### Acknowledgements

This work was supported by the Air Force through the Geophysics Directorate of the Phillips Laboratory under contract F19628-90- K-0011. The field work was made possible through a collaborative effort with scientists from NOAA, the Atmospheric Science Laboratory (ASL) at WSMR, and NASA. The participants were: B.A. Bodhaine, J.F. Boatman, J.J. Deluisi, Y. Kim, M.J. Post, R.C. Schnell, P.J. Sheridan, and D.M. Garvey.

The names of the scientists and engineers from the University of Wyoming who worked on this project are as follows: J.M. Rosen (PI) and N.T. Kjome (Research Scientist).

The work described here has not been published as part of any previous contract.

#### References

Baumgardner, D., B. Huebert, and C. Wilson, Meeting Review: Airborne Aerosol Inlet Workshop, NCAR Tech. Rep. NCAR/TN-362+1A, Research Aviation Facility, Boulder, CO, 1991.

Bodhaine, B.A., and M.E. Murphy, Calibration of an automatic condensation nuclei counter at the South Pole, *J. Aerosol Sci.*, 11, 305-312, 1980.

Bodhaine, B.A., J.J. Deluisi, J.F. Boatman, M.J. Post and J.M. Rosen, The front range lidar, aircraft, and balloon experiment, NOAA Data Rep. ERL CMDL-2, Climate Monitoring and Diagnostics Laboratory, Boulder, CO, 27 pp., 1990.

Bodhaine, B.A., J.J. Deluisi, J.F. Boatman, Y. Kim, D.L. Wellman, R.L. Gunter, M.J. Post, R.E. Cupp, T. McNice, J.M. Rosen, P.J. Sheridan, R.C. Schnell, D.M. Garvey, A.E. Wade, R.G. Steninhoff, The second front range lidar, aircraft and balloon experiment, NOAA Data Report ERL CMDL-8, Climate Monitoring and Diagnostics Laboratory, Boulder, Colorado. 142 pp., (available through NTIS), 1991a.

Bodhaine, B.A., N.C. Ahlquist, and R.C. Schnell, Three-wavelength nephelometer suitable for aircraft measurement of background aerosol scattering coefficient, *Atmos. Environ.*, 25A, 2267-2276, 1991b.

Bowdle, D.A., J. Rothermel, J.M. Vaughan, D.W. Brown, and M.J. Post, Aerosol backscatter measurements at 10.6 micrometers with airborne and ground-based CO<sub>2</sub> doppler lidars over the Colorado high plains 1. Lidar intercomparison, *J. Geophys. Res.*, 96, 5327-5335, 1991.

DeLuisi, J.J., R.K. Sato, and D.A. Gillette, On the sensitivity of errors in calculated Mie optical cross sections due to errors in samplings of Junge-type aerosol size distributions, *Atmos. Envir.*, 10, 717-721, 1976.

Garvey, D.M., and R.G. Pinnick, Calibration of Knollenberg FSSP light-scattering counters for measurement of cloud droplets, *Aerosol Sci. Technol.*, 2, 477-487, 1983.

- Hansen, A.D.A., and H. Rosen, The aethalometer - an instrument for the real-time measurement of optical absorption by aerosol particles, *Sci. Total Environ.*, 36, 191-196, 1984.
- Horvath, H., R.L. Gunter and S.W. Wilkison, Determination of the coarse mode of the atmospheric aerosol using data from a forward- scattering spectrometer probe, *Aer. Sci. Technol.*, 12, 964-980, 1990.
- Kent, G.S., and G.K. Yue, The modeling of CO<sub>2</sub> lidar backscatter from stratospheric aerosols, *J. Geophys. Res.*, 96, 5279-5292, 1991.
- Kent, G.S., G.K. Yue, U.G. Farrukh, and A. Deepak, Modeling atmospheric backscatter at CO<sub>2</sub> laser wavelengths. 1. Aerosol properties, modeling techniques, and associated problems, *Appl. Opt.*, 22, 1655-1678, 1983.
- Kim, Y.J. and J.F. Boatman, Size calibration corrections for the active scattering aerosol spectrometer probe (ASASP-100X), *Aer. Sci. Technol.*, 12, 665-672, 1990a.
- Kim, Y.J. and J.F. Boatman, Size calibration corrections for the forward scattering spectrometer probe (FSSP) for measurement of atmospheric aerosols of different refractive indices, *J. Atmos. Oceanic Technol.*, 7, 681-688, 1990b.
- Lijura, Y., N. Sugimoto, Y. Sasano, and H. Shimzu, Improvement of lidar data processing for stratospheric aerosol measurements, *Appl. Opt.*, 26, 5299-5306, 1987.
- Pinnick, R.G. and J.J. Auvermann, Response characteristics of Knollenberg light-scattering aerosol counters, *J. Aerosol Sci.*, 10, 55-74, 1979.
- Pinnick, R.G., and J.M. Rosen, Response of Knollenberg light- scattering counters to non-spherical doublet polystyrene latex aerosols, *J. Aerosol Sci.*, 10, 533-538, 1979.
- Post, M.J., Aerosol backscattering profiles at CO<sub>2</sub> wavelengths: the NOAA data base, *Appl. Opt.*, 15, 2507-2509, 1984.
- Rosen, J.M. and N.T. Kjome, Backscattersonde: A new instrument for atmospheric aerosol research, *Appl. Opt.*, 30, 1552-1561, 1991.
- Russell, P.B., T.J. Swissler, and M.P. McCormick, Methodology for error analysis and simulation of lidar aerosol measurements, *Appl. Opt.*, 18, 3783-3799, 1979.
- Sheridan, P.J., R.C. Schnell, J.B. Kahl, F.F. Boatman, D.M. Garvey, Micro-analysis of the aerosol collected over south central New Mexico during the ALIVE field experiment May-December 1989, *Atmos. Env.*, in press, 1991.
- Shettle, E.P., and R.W. Fenn, Models for the aerosols of the lower atmosphere and the effects of humidity variations on their optical properties, *Env. Res. Paper No. 676*, AFGL-TR-79-0214, Air Force Geophysics Lab, Hanscom, Mass., 1979, ADA085951.
- Spinhirne, J.D., J.A. Reagan, and B.M. Herman, Vertical distribution of aerosol extinction cross section and inference of aerosol imaginary index in the troposphere by lidar technique, *J. Appl. Meteorol.*, 19, 426-438, 1980.

Wellman, D.L., M. Luria, C.C. Van Valin, and J.F. Boatman, The use of an airborne air sampling platform for regional air quality studies, NOAA Tech. Rep. ERL 437-ARL 10, Air Resources Laboratory, Boulder, Colorado, 1989.



**Table 1**  
**Carbon Composition of Aerosols**  
**(percent by mass)**

Layer	23 May 90	24 may 90
1	3.0	5.0
2	3.8	3.0
3	1.5	0.6
4	0.8	3.0
5	1.3	0.9
6	1.0	0.5

**Table 2**  
**Ensemble of Refractive Indices**  
**Used in Calculations**

Index of Refraction	Possible Aerosol
1.33 - 0.000i	Water
1.49 - 0.000i/0.006i	Sea Salt
1.50 - 0.000i/0.006i	Rural (70% RH)
1.52 - 0.000i/0.006i	Rural (50% RH)
	Ammonium Sulfate
1.53 - 0.000i/0.006i	Rural (0% RH)
	Dust-like
1.59 - 0.000i	Polystyrene Spheres (for calibration)

**Table 3**  
**Optimal Choice Refractive Index**

Layer	26 July 89	23 May 90	24 May 90
1	1.49-0.000i	1.49-0.000i	1.49-0.000i
2	1.53-0.000i	1.49-0.000i	1.49-0.000i
3	1.49-0.000i	1.49-0.000i	1.59-0.000i
4	1.50-0.006i	1.52-0.006i	1.49-0.000i
5		1.49-0.000i	1.49-0.000i
6		1.49-0.000i	1.49-0.000i

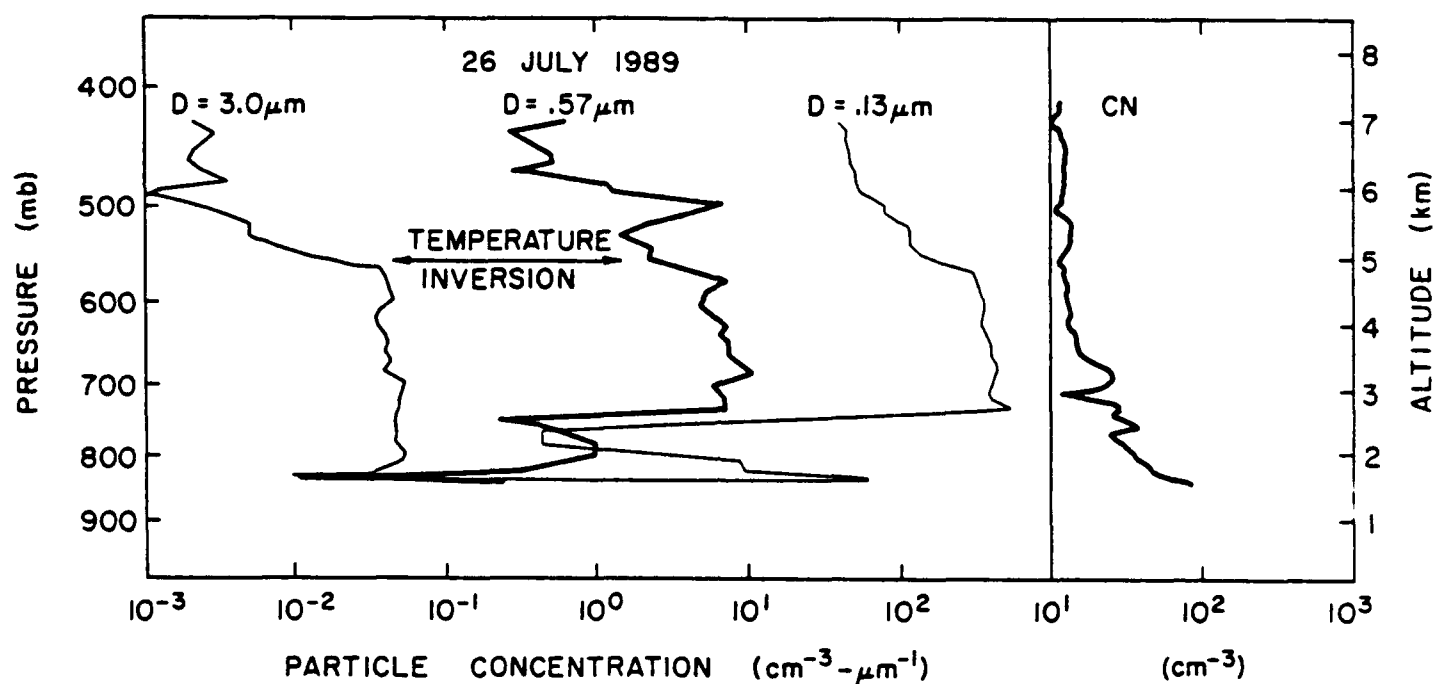


**Figure 1. Particle concentration profiles obtained on aircraft ascent during the first field experiment on 26 July 1989.**

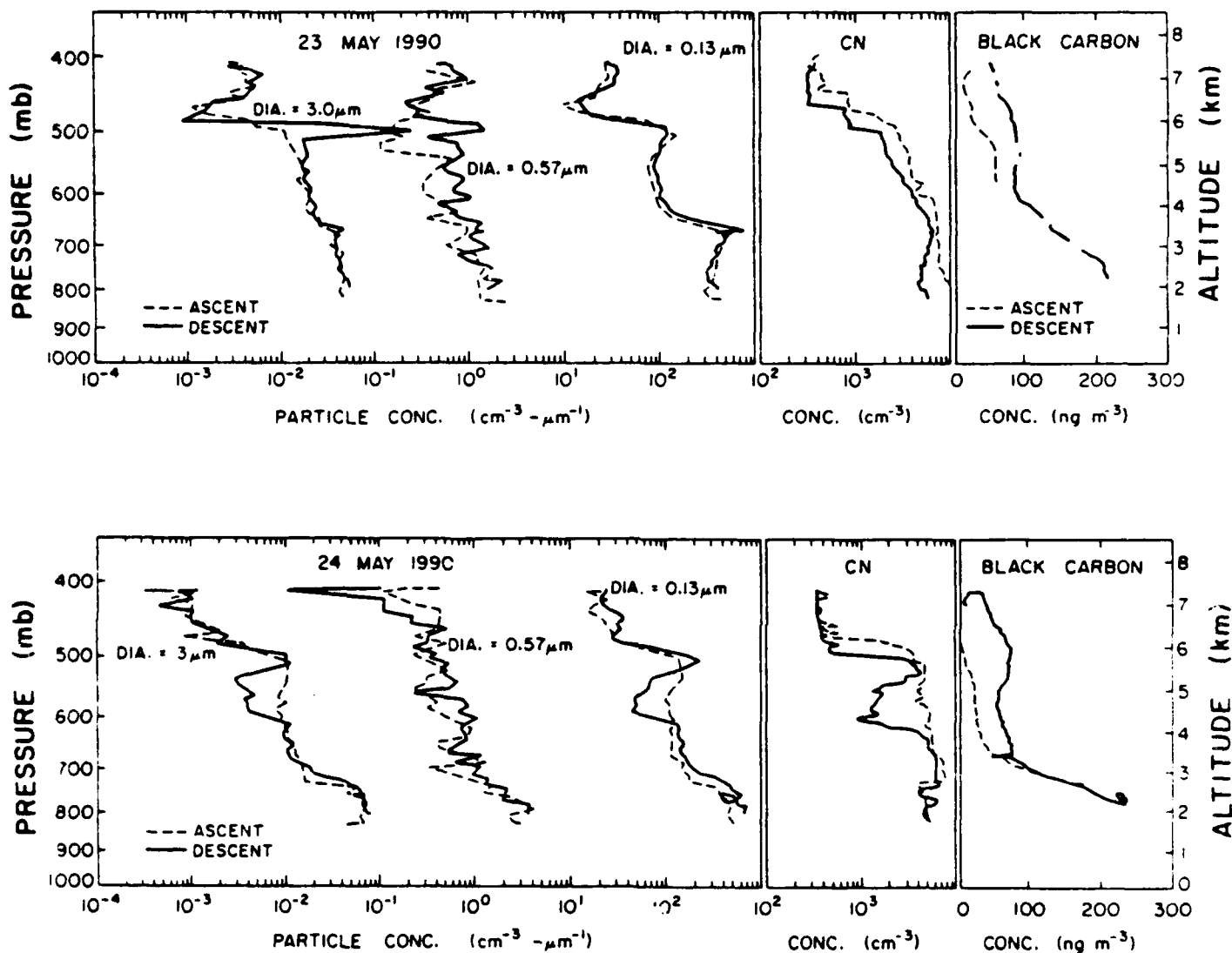


**Figure 2. Particle, condensation nuclei (CN), and black carbon concentration profiles obtained on aircraft ascent and descent during the second field experiment in May 1990.**

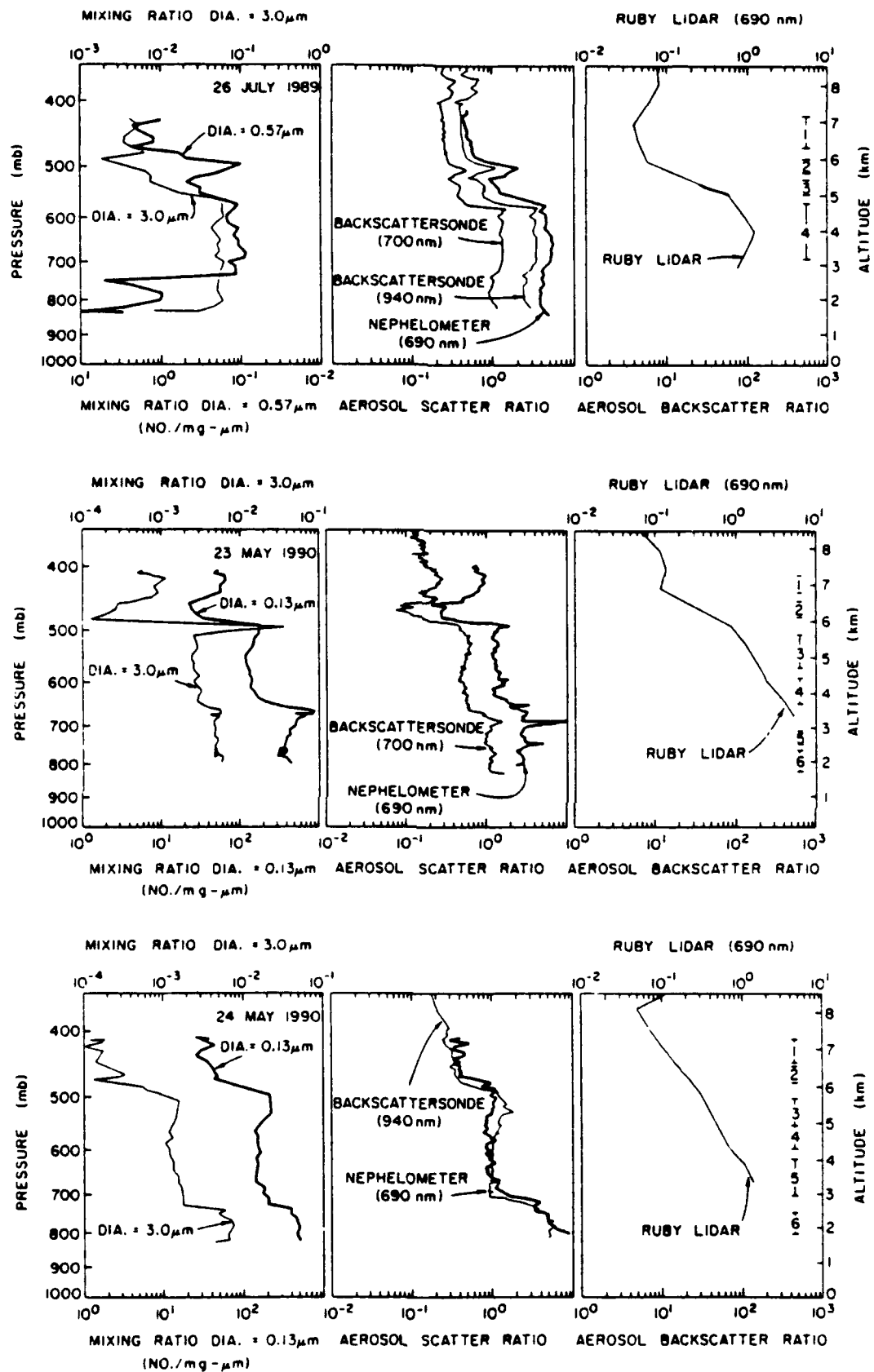
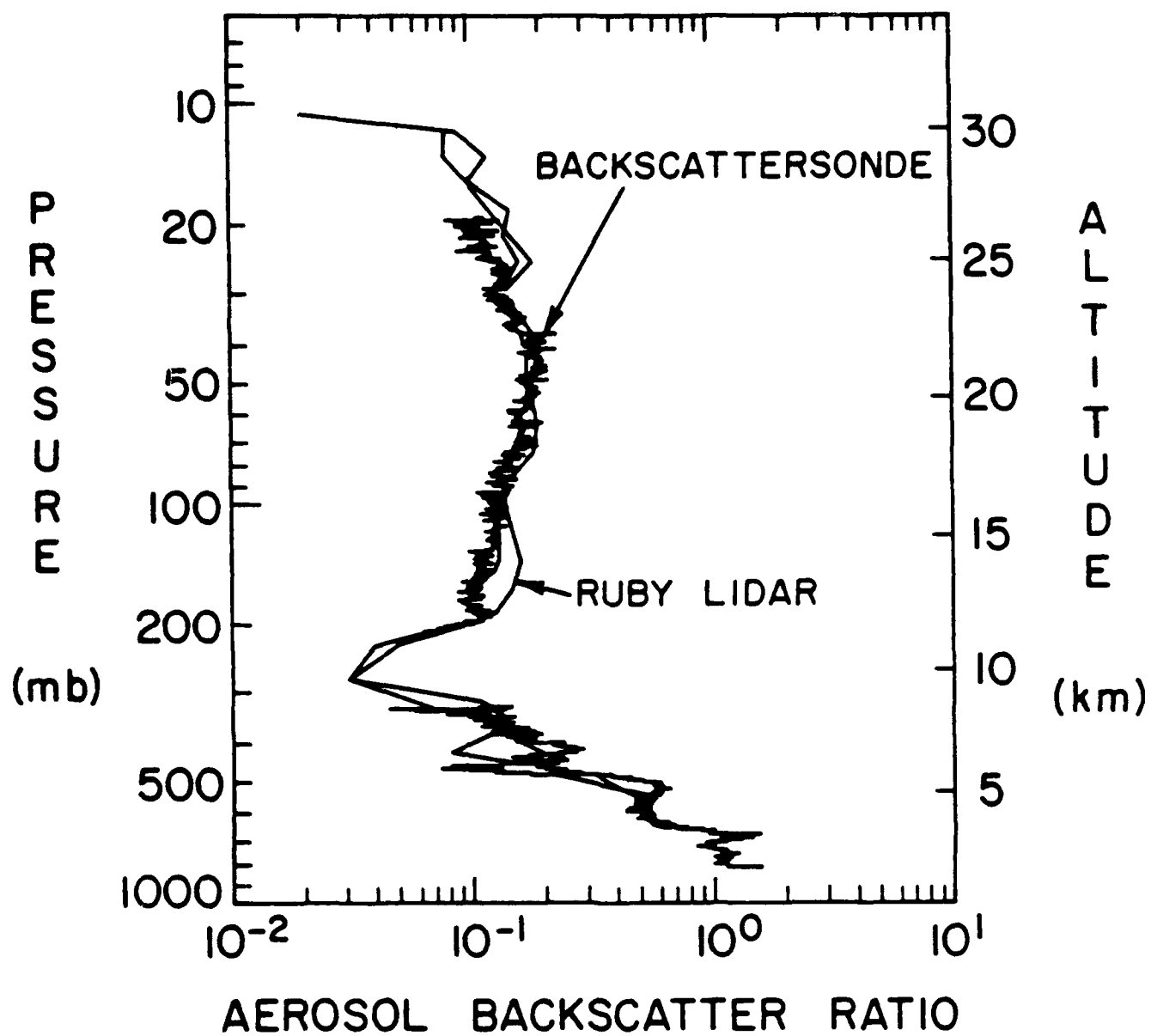


Figure 3. Particle concentration and optical scattering profiles obtained for the aerosols present during the field measurements.



**Figure 4. A comparison of the backscattersonde and ruby lidar profiles for the 1989 experiment period.**

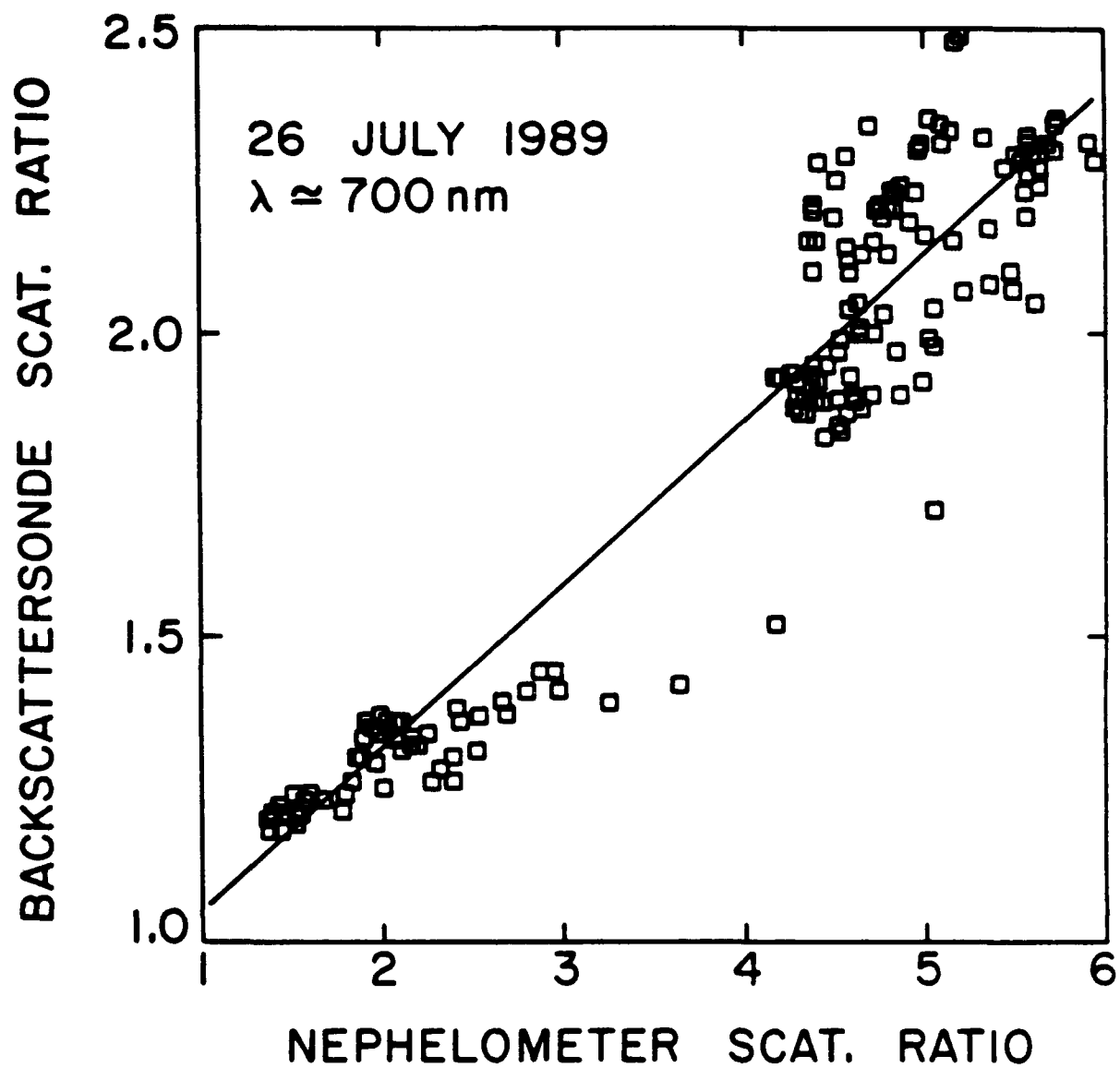


Figure 5. A scatter plot of the backscattersonde vs. nephelometer measurements averaged over 2 mb altitude increments for the 26 July experiment.

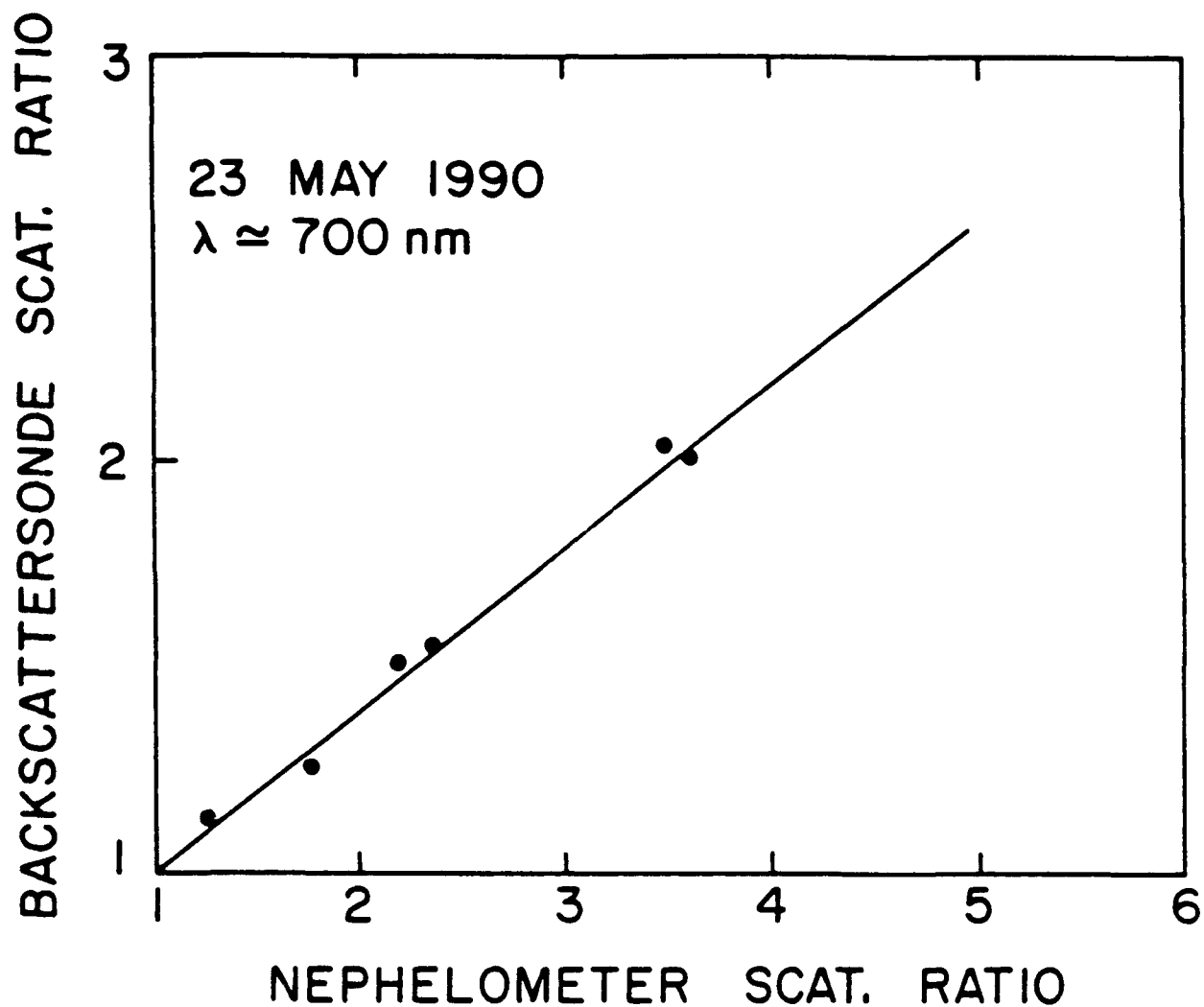


Figure 6. The relation between the backscattersonde and nephelometer measurements for the six layers defined in Figure 3 for the May 1990 experiment period.

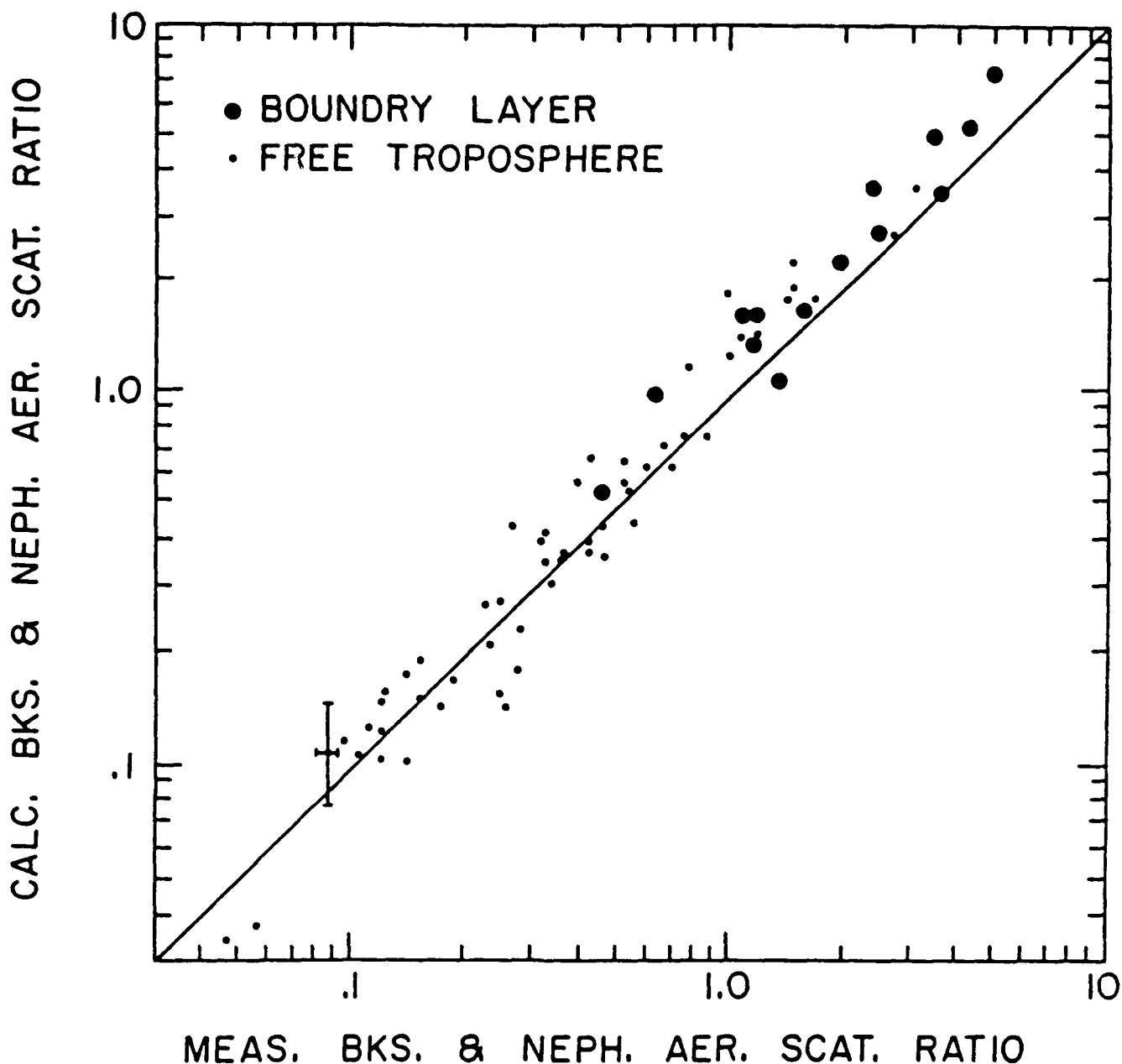


Figure 7. A summary scatter plot of the agreement between the calculated and measured nephelometer and backscatterer aerosol scatter ratios for all wavelengths. The coordinate of every point is derived from the measured and calculated value for the nephelometer at one of its three wavelengths or the backscatterer at one of its two wavelengths for the layers defined in Figure 3. The magnitude of the uncertainty is demonstrated on one point but applies to all points. The solid line represents calculated = measured values.